Proc. IEEE Data Compression Conference, pages 83-91, April 2-4, 2002, Snowbird, UT, USA.

Combining FEC and Optimal Soft-Input Source Decoding for the Reliable Transmission of Correlated Variable-Length Encoded Signals

Jörg Kliewer and *Ragnar Thobaben*

University of Kiel
Institute for Circuits and Systems Theory
Kaiserstr. 2, 24143 Kiel, Germany
Phone: +49-431-880-6130, Fax: +49-431-880-6128
E-Mail: {jkl, rat}@tf.uni-kiel.de

Abstract

In this paper we utilize both the implicit residual source correlation and the explicit redundancy from a forward-error-correction (FEC) scheme for the error protection of packetized variable-length encoded source indices. The implicit source correlation is exploited in a novel symbol-based soft-input a-posteriori probability (APP) decoder, which leads to an optimal decoding process in combination with a mean-squares or maximum a-posteriori probability estimation of the reconstructed source signal. When additionally the variable-length encoded source data is protected by channel codes, an iterative source-channel decoder can be obtained in the same way as for serially concatenated codes, where the outer constituent decoder is replaced by the proposed APP source decoder. Simulation results show that by additionally considering the correlations between the variable-length encoded source indices the error-correction performance can be highly increased.

1 Introduction

Recently, the reliable transmission of variable-length encoded source signals over wireless channels has attained much interest, since many source compression standards employ variable-length codes (VLCs), and since there is also a high demand for mobile access of multimedia data in current and future wireless systems. Some of these approaches [1–5] focus on robust decoding of such variable-length encoded streams using joint source-channel decoding techniques. Whereas [2, 3, 5] use a first-order Markov model for the source and thus incorporate residual redundancy into the decoding process, [1, 4] model the source indices as uncorrelated. In [4] a trellis representation for VLCs is presented, where the BCJR algorithm [6] is utilized for soft-input a-posteriori probability (APP) decoding.

In the following we propose a joint source-channel decoding approach for packetized variable-length encoded source indices, which is based on the VLC trellis representation from [4]. As a new result we show for the first-order Markov source model that by modification of the BCJR algorithm the source correlation can be included in the VLC trellis.

This leads to a novel soft-input source decoding algorithm, which uses the implicit residual redundancy after source encoding and the bit-reliability information for the whole packet at the channel output in order to protect the variable-length encoded source indices. In combination with a subsequent mean-squares [7] or maximum a-posteriori probability (MAP) estimation the proposed index-based APP VLC source decoder is optimal. Furthermore, when the resulting bitstream is additionally protected by a channel code, the APP VLC decoder can be used as constituent decoder in an iterative decoding scheme, which will be demonstrated in the second part of this paper.

2 Transmission System

Let us consider the block diagram of the transmission system depicted in Fig. 1. One packet $\mathbf{U} = [U_1, U_2, \ldots, U_K]$ of the source signal consists of K source symbols U_k, where k denotes the sample index. After subsequent (vector-) quantization, the resulting indices $I_k \in \mathcal{I}$ from the finite alphabet $\mathcal{I} = \{0, 1, \ldots, 2^M - 1\}$ are represented with M bits. We can generally assume that there is a certain amount of redundancy in the index vector $\mathbf{I} = [I_1, I_2, \ldots, I_K]$ due to delay and complexity constraints for the quantization stage. In the following the correlation between the indices I_k is modeled by a first-order stationary Markov process with index transition probabilities $P(I_k = \lambda \,|\, I_{k-1} = \mu)$ for $\lambda, \mu = 0, 1, \ldots, 2^M - 1$.

The VLC encoder in Fig. 1 now maps each fixed-length index I_k to a variable-length bit vector $\mathbf{c}(\lambda) = \mathcal{C}(I_k = \lambda)$ using the prefix code $\mathcal{C}$. This leads to a binary sequence $\mathbf{w} = [w_1, w_2, \ldots, w_N]$ of length N where w_n represents a single bit at bit index n. Then

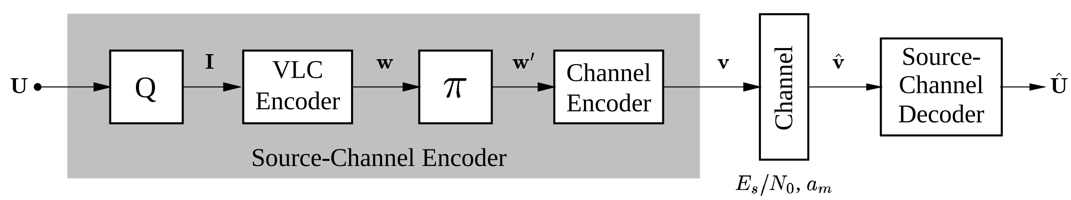

Figure 1: Model of the transmission system

the bitstream $\mathbf{w}$ is interleaved in order to provide uncorrelated bits for the rate-R channel encoder. The resulting codewords form the vector $\mathbf{v}$, which is transmitted over a fully interleaved flat Rayleigh channel, where we assume coherently detected binary phase-shift keying (BPSK) for the modulation. The conditional p.d.f. of the received soft-bit $\hat{v}_m \in \mathbb{R}$, $m = 1, 2, \ldots, N/R$, at the channel output given the transmitted bit $v_m \in \{0, 1\}$ can be written as

$$p(\hat{v}_m \,|\, v_m) = \frac{1}{\sqrt{2\pi}\sigma_e} \cdot e^{-\frac{1}{2\sigma_e^2}(\hat{v}_m - a_m \cdot \bar{v}_m)^2} \quad \text{with} \quad \bar{v}_m = 1 - 2 \cdot v_m. \tag{1}$$

Herein, $\sigma_e^2 = \frac{N_0}{2E_s}$ denotes the channel noise variance where E_s is the energy to transmit each bit and N_0 the one-sided power spectral density of the noise, and the variable a_m

represents the Rayleigh-distributed attenuation factor. Eq. (1) can also be expressed using the conditional log-likelihood ratios (L-values) [8]

$$L(\hat{v}_m \mid v_m) = \log\left(\frac{p(\hat{v}_m \mid v_m = 0)}{p(\hat{v}_m \mid v_m = 1)}\right) = 4\,\frac{E_s}{N_0}\,a_m\,\hat{v}_m = L_c\,a_m\,\hat{v}_m \quad \text{with} \quad L_c = 4\,\frac{E_s}{N_0}. \tag{2}$$

If $a_m = 1$ for all m we have the special case of an additive white Gaussian noise (AWGN) channel.

3 Optimal Soft-Input Source Decoding

In this section we only deal with the error correcting capabilities of the implicit residual source redundancy after quantization and derive a soft-input APP decoder for the resulting variable-length encoded sequence. Thus, in this special case our general source-channel encoder in Fig. 1 just contains the quantizer and the VLC encoder, and we therefore have $\mathbf{v} = \mathbf{w}$.

3.1 Trellis representation

The proposed decoding technique is based on the VLC trellis representation derived by Bauer and Hagenauer in [4], where an example is given in Fig. 2 for $K = 5$, $N = 10$ and the Huffman code

$$\mathcal{C} = \{\mathbf{c}(0)=[1],\ \mathbf{c}(1)=[0,1],\ \mathbf{c}(2)=[0,0,0],\ \mathbf{c}(3)=[0,0,1]\}.$$

Note that we have a time-variant trellis with a diverging, a stationary, and a converging section. The states $S_k = n$, where S_k refers to the state at time instant k and n denotes

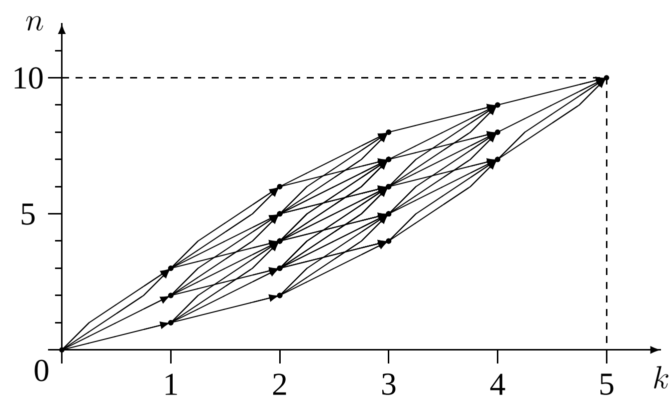

Figure 2: Trellis representation for $K = 5$, $N = 10$ and $\mathcal{C} = \{\mathbf{c}(0) = [1],\ \mathbf{c}(1) = [0,1],\ \mathbf{c}(2)=[0,0,0],\ \mathbf{c}(3)=[0,0,1]\}$ [4]

its value, correspond to the nodes of the trellis in Fig. 2. They represent all possible bit positions for a given k in the variable-length encoded bit sequence $\mathbf{w}$. In the following we denote this set of all possible states $S_k = n$ as $\mathcal{N}_k$. The transition from state $S_{k-1} = n_1$ to

$S_k = n_2$ is caused by the source symbol $I_k = \lambda$, $\lambda \in \mathcal{I}$, and the corresponding Huffman codeword $\mathbf{c}(\lambda)$ with length $l(\mathbf{c}(\lambda)) = n_2 - n_1$, respectively. A code-table, which contains two or more codewords having the same length l, leads to parallel transitions between the states $S_{k-1} = n_1$ and $S_k = n_2$ in the VLC trellis (see Fig. 2).

3.2 A-posteriori probabilities

We are now interested in deriving the a-posteriori probabilities $P(I_k = \lambda \,|\, \hat{\mathbf{v}})$, where the source correlation modeled by the index transition probabilities $P(I_k = \lambda \,|\, I_{k-1} = \mu)$ of the Markov model is included in the decoding algorithm.

In a first step the APPs $P(I_k = \lambda \,|\, \hat{\mathbf{v}})$ can be decomposed analog to the BCJR algorithm [6] as

$$P(I_k = \lambda \,|\, \hat{\mathbf{v}}) = \frac{1}{C} \sum_{n_2 \in \mathcal{N}_k} \sum_{n_1 \in \mathcal{N}_{k-1}} \underbrace{p(\hat{\mathbf{v}}_{n_2+1}^{N} \,|\, S_k = n_2)}_{=:\,\beta_k(n_2)} \cdot \cdot \underbrace{p(\hat{\mathbf{v}}_{n_1+1}^{n_2}, I_k = \lambda, S_k = n_2 \,|\, S_{k-1} = n_1, \hat{\mathbf{v}}_1^{n_1})}_{=:\,\gamma_k(\lambda, n_2, n_1)} \cdot \underbrace{p(S_{k-1} = n_1, \hat{\mathbf{v}}_1^{n_1})}_{=:\,\alpha_{k-1}(n_1)}, \quad (3)$$

where a subsequence from bit position a to b of the vector $\hat{\mathbf{v}}$ is denoted as $\hat{\mathbf{v}}_a^b = [\hat{v}_a, \hat{v}_{a+1}, \ldots, \hat{v}_b]$. The constant $C = p(\hat{\mathbf{v}})$ in (3) ensures that the $P(I_k = \lambda \,|\, \hat{\mathbf{v}})$ are true probabilities.

The term $\alpha_{k-1}(n_1)$ from (3) can be written as a forward recursion according to [6]

$$\alpha_k(n_2) = \sum_{n_1 \in \mathcal{N}_{k-1}} \sum_{\lambda=0}^{2^M-1} \gamma_k(\lambda, n_2, n_1) \cdot \alpha_{k-1}(n_1), \quad \alpha_0(0) = 1. \quad (4)$$

It can now be shown that by including the first-order Markov model for the quantized indices we can derive the following expression for the term $\gamma_k(\lambda, n_2, n_1)$:

$$\gamma_k(\lambda, n_2, n_1) = \underbrace{p(\hat{\mathbf{v}}_{n_1+1}^{n_2} \,|\, I_k = \lambda)}_{\text{channel term}} \sum_{\mu=0}^{2^M-1} \underbrace{P(I_k = \lambda, S_k = n_2 \,|\, I_{k-1} = \mu, S_{k-1} = n_1)}_{\text{transition probability on the trellis (Markov source)}} \cdot \cdot \underbrace{\frac{1}{C_1(n_1)} \gamma_{k-1}(\mu, n_1, n_0)\, \alpha_{k-2}(n_0)}_{\text{"forward" APP } P(I_{k-1} = \mu \,|\, S_{k-1} = n_1, \hat{\mathbf{v}}_1^{n_1})} \quad (5)$$

with $n_0 = n_1 - l(\mathbf{c}(\mu))$ and $C_1(n_1)$ denoting a constant depending on n_1. Herein, the conditional probability $P(I_k = \lambda, S_k = n_2 \,|\, I_{k-1} = \mu, S_{k-1} = n_1)$ represents the transition probability of the Markov source according to

$$P(I_k = \lambda, S_k = n_2 \,|\, I_{k-1} = \mu, S_{k-1} = n_1) = \frac{1}{C_2(n_1, \mu)} \begin{cases} P(I_k = \lambda \,|\, I_{k-1} = \mu) & \text{for } n_2 - n_1 = l(\mathbf{c}(\lambda)), \\ 0 & \text{otherwise,} \end{cases} \quad (6)$$

with the normalization factor $\quad C_2(n_1,\mu) = \sum_{n_2' \in \mathcal{N}_k} \sum_{\substack{\lambda \in \mathcal{I}: \\ l(\mathbf{c}(\lambda)) = n_2' - n_1}} P(I_k = \lambda \,|\, I_{k-1} = \mu).$

The normalization takes into account that in both the stationary and the converging region of the VLC trellis not all transitions from $S_{k-1} = n_1$ to $S_k = n_1 + l(\mathbf{c}(\lambda))$ for $\lambda = 0, 1, \ldots, 2^M - 1$ are possible anymore. This can for instance be observed in the example from Fig. 2 for all states with $k = 4$. We can see from (5) that $\gamma_k(\lambda, n_2, n_1)$, which can be considered as a weighting term for the trellis branches, now contains three different types of information, namely the bit-reliability information from the channel, a-priori knowledge about the correlation between source indices for time instants $k-1$ and k, and *index-based* reliability values for the time instant $k-1$. This can be regarded as an extension of the BCJR forward recursion (4) for variable-length encoded first-order Markov sources.

The term $\beta_k(n_2)$ in (3) is obtained with the backward recursion from [6]:

$$\beta_k(n_1) = \sum_{n_2 \in \mathcal{N}_{k+1}} \sum_{\lambda=0}^{2^M - 1} \beta_{k+1}(n_2) \cdot \gamma'_{k+1}(\lambda, n_2, n_1), \quad \beta_K(N) = 1, \quad \text{with} \tag{7}$$

$$\gamma'_{k+1}(\lambda, n_2, n_1) = \underbrace{p(\hat{\mathbf{v}}_{n_1+1}^{n_2} \,|\, I_{k+1} = \lambda)}_{\text{channel term}} \cdot \underbrace{P(I_{k+1} = \lambda, S_{k+1} = n_2 \,|\, S_k = n_1)}_{\text{source prob. distribution on the trellis}}. \tag{8}$$

In contrast to (5) here only the probability distribution of the source indices is considered, which can be adapted to the VLC trellis with a similar normalization as in (6).

We now have all parameters available in order to calculate the APPs $P(I_k = \lambda \,|\, \hat{\mathbf{v}})$ for $\lambda = 0, 1, \ldots, 2^M - 1$ according to (3). Note that when the APPs $P(I_k = \lambda \,|\, \hat{\mathbf{v}})$ are used for optimally estimating the reconstructed values U_k at the decoder output, which can for example be carried out with a mean-squares or MAP estimation, the whole decoding process is optimal in the mean-squares or MAP sense.

4 Iterative Decoding with Channel Codes

Due to the high sensitivity of the variable-length encoded bitstream to channel noise, using only the residual source redundancy for error protection may not be enough in many cases. Therefore, in the following we assume that the interleaved output of the VLC encoder is protected by a systematic (convolutional) channel code prior to transmission, as it is depicted in Fig. 1. Since this encoding scheme is highly similar to a serially concatenated code, however, with the difference that the redundancy provided by the first channel encoder is replaced with the residual source redundancy, we can apply a similar iterative decoding strategy [9]. In this decoding scheme the outer constituent decoder is replaced by the soft-input APP source decoder from the last section.

Fig. 3 shows the structure of the proposed decoder. The APP channel decoder calculates reliability information for the variable-length encoded index-bits using the conditional L-values

$$L^{(C)}(w'_n) = \log\left(\frac{P(w'_n = 0 \,|\, \hat{\mathbf{v}})}{P(w'_n = 1 \,|\, \hat{\mathbf{v}})}\right) = L_c\, a'_n\, \hat{w}'_n + L_a^{(C)}(w'_n) + L_{\text{extr}}^{(C)}(w'_n)$$

for $n = 1, 2, \dots, N$. $L_c\, a'_n\, \hat{w}'_n$ is defined analog to (2) for the interleaved index-bits w'_n and the corresponding Rayleigh factors a'_n, $L_a^{(C)}(w'_n)$ denotes the a-priori information for the index-bit w'_n, and $L_{\text{extr}}^{(C)}(w'_n)$ refers to the extrinsic information [8]. After subtraction of the a-priori term and after deinterleaving we obtain the L-values $L_{\text{e}}^{(C)}(w_n) = L_c\, a_n\, \hat{w}_n + L_{\text{extr}}^{(C)}(w_n)$, which are used as a-priori information $L_a^{(S)}(w_n) = L_e^{(C)}(w_n)$ for the VLC source decoder. Since we assume that all bits are uncorrelated the index-based p.d.f. $p(\hat{\mathbf{w}}_{n_1+1}^{n_2} \,|\, I_k = \lambda)\, P_{\text{extr}}(I_k = \lambda \,|\, \hat{\mathbf{v}})$ for $\lambda \in \mathcal{I}$ is obtained by bitwise multiplication of the p.d.f.s for the corresponding index-bits, which are calculated from the a-priori L-values $L_a^{(S)}(w_n)$. The extrinsic probability $P_{\text{extr}}(I_k = \lambda \,|\, \hat{\mathbf{v}})$ for $\lambda \in \mathcal{I}$ is then used as an extra weighting term in (5) and (8), respectively. The APP source

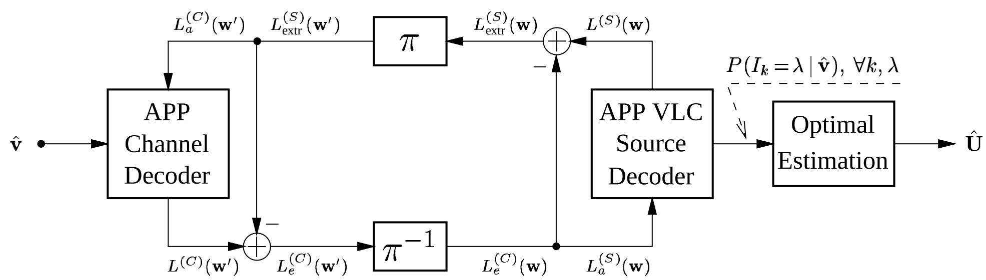

Figure 3: Iterative joint source-channel decoder

decoder now issues index-based APPs $P(I_k = \lambda \,|\, \hat{\mathbf{v}})$, where the corresponding bit-based probabilities can be calculated according to

$$P(w_n = i \,|\, \hat{\mathbf{v}}) = \frac{1}{C} \sum_{\substack{(k,n_1,\lambda) \in (\mathcal{K}_n \times \mathcal{N}_{k-1} \times \mathcal{I}): \\ w_n = i}} \beta_k(n_2)\, \gamma_k(\lambda, n_2, n_1)\, \alpha_{k-1}(n_1) \qquad (9)$$

with $\mathcal{K}_n$ denoting the set of all possible states for bit position n. Note that the summation in (9) is carried out over all trellis branches, which correspond to bit $w_n = i \in \{0, 1\}$ at bit position n. By subtracting the source a-priori information $L_a^{(S)}(w_n)$ from the resulting L-values $L^{(S)}(w_n)$ we finally obtain the extrinsic information $L_{\text{extr}}^{(S)}(w_n)$, which is used as a-priori information in the next channel decoding round.

5 Simulation Results

In order to assess the performance of the proposed decoding technique, simulations are carried out for the BPSK-modulated fully interleaved flat Rayleigh channel, where the attenuation factors a_n and the channel signal-to-noise ratio (SNR) are assumed to be ideally estimated. As variable-length code we utilize a standard Huffman code, and the source redundancy is modeled by an AR(1) process with correlation coefficient $a = 0.9$ quantized with $M = 4$ bits by an uniform scalar quantizer. After variable-length encoding the resulting bitstream is interleaved using an S-random interleaver [10].

The channel code utilized in the simulations is a terminated rate-$3/4$ recursive systematic convolutional (RSC) code, which is obtained from a memory-4 rate-$1/2$ mother code with generator polynomials $(g_0, g_1)_8 = (35, 23)_8$ by puncturing with the pattern $[1, 1, 1; 1, 0, 0]$.

For the simulations we use packets of length $K = 100$ over 50 different realizations of the source signal, where each packet is interleaved and transmitted independently. Besides, each of these 50 packets is averaged over 100 channel realizations. The source transition probabilities $P(I_k = \lambda \,|\, I_{k-1} = \mu)$ are obtained from a large training set of source realizations. We furthermore assume that the sensitive parameters N and K are protected by a strong channel code and thus, are transmitted without errors to the decoder.

The simulation results for the Rayleigh channel are depicted in Fig. 4. Fig. 4(a) considers a MAP estimation of the APPs $P(I_k = \lambda \,|\, \hat{\mathbf{v}})$, where the symbol error rate (SER) is plotted over the channel parameter E_b/N_0 with $E_b = E_s/R$.

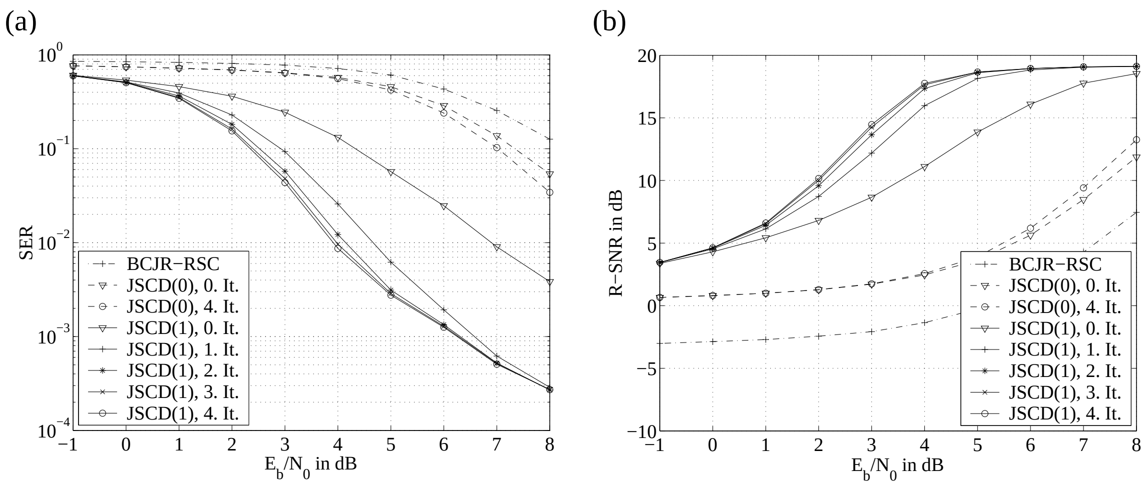

Figure 4: Simulation results for the fully interleaved flat Rayleigh channel ($K = 100$ for 50 different realizations of the source signal, each averaged over 100 channel realizations; $M = 4$, AR(1) process with source correlation $a = 0.9$): (a) MAP estimation and symbol error rate (SER), (b) mean-squares estimation and reconstruction SNR (R-SNR).

Both the ”JSCD(0)” and ”JSCD(1)” techniques employ the iterative joint source-channel decoder from Section 4. However, the ”JSCD(0)” approach only exploits the probability distribution of the source indices and hence, basically corresponds to the method presented in [4], whereas the ”JSCD(1)” technique also utilizes the mutual residual source correlation between the indices I_k and contains the soft-input APP decoder from Section 3. Protecting the variable-length encoded bitstream only with the rate-$3/4$ RSC channel code without considering any source statistics leads to the ”BCJR-RSC” method, which employs the BCJR algorithm as channel decoder. In order to allow a fair comparison, all approaches have the same overall bandwidth on the transmission channel.

As we can see from Fig. 4(a), by incorporating the residual source correlation into the decoding process, for $E_b/N_0 \geq 5\,$dB we achieve a SER for the ”JSCD(1)” approach being at least one order of magnitude lower than that for the ”JSCD(0)” technique, even if only the first half-iteration (”zero-th” iteration) is carried out. However, increasing the number of iterations over three, a further gain is only observed in the ”waterfall” region of the SNR-SER relation in Fig. 4(a).

Fig. 4(b) shows the results for a mean-squares estimation [7] of the reconstructed source signal, where now the reconstruction SNR (R-SNR) is used as error measure. We can see from Fig. 4(b) that with iterative joint source-channel decoding we almost achieve clear channel quality for $E_b/N_0 > 4\,$dB. This verifies the good performance of the proposed transmission system.

Finally, we consider a more practical example where the Huffman-encoded one-dimensional lowpass subband signal of a three-level wavelet decomposition for the ”Lena” image is transmitted over an AWGN channel. From the results in Fig. 5 it can be observed that also for real data the ”JSCD(1)” technique leads to an improved decoding performance.

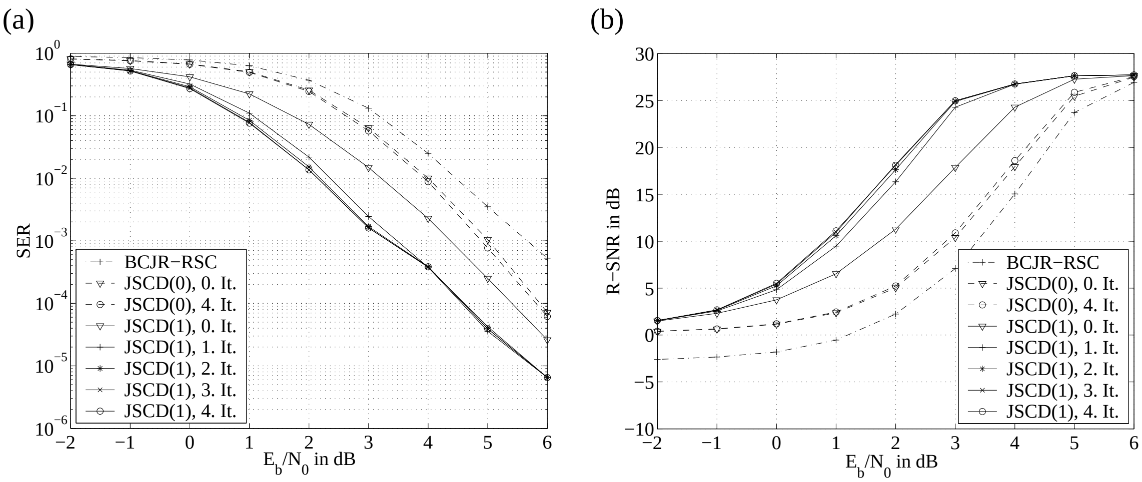

Figure 5: Simulation results for the lowpass subband signal of a wavelet-decomposed ”Lena” image (AWGN channel; $K = 64$, averaged over 75 channel realizations; $M = 5$): (a) MAP estimation and symbol error rate (SER), (b) mean-squares estimation and reconstruction SNR (R-SNR).

6 Acknowledgment

The authors would like to thank Dr. Norbert Görtz for providing some parts of the simulation software related to APP channel decoding.

7 Conclusion

As a novelty we have shown that by starting from the classical BCJR algorithm an optimal soft-input APP-based decoding technique for packetized variable-length encoded correlated source indices can be derived by modification of the forward recursion and adaptation to the non-stationary VLC trellis. Besides the transition probabilities of the underlying first-order Markov model and some knowledge about the transmission channel, also the number of source symbols and the number of bits in the packet are used as a-priori information in the decoding process. When the variable-length encoded bitstream is additionally protected by channel codes, an iterative decoder consisting of an APP decoder for the channel code and the proposed APP VLC source decoder can be derived in the same manner as for serially concatenated codes. The simulation results show that by exploiting residual index correlations in the decoding process after variable-length source encoding, the reconstruction quality can be highly improved. For example, for a fully interleaved flat Rayleigh channel and a mean-squares estimation of the reconstructed source symbols the iterative source-channel decoder almost leads to clear-channel quality for an E_b/N_0 being larger than 4 dB.

References

[1] J. Wen and J. D. Villasenor, "Utilizing soft information in decoding of variable length codes," in *Proc. Data Compression Conference*, Snowbird, UT, USA, Mar. 1999, pp. 131–139.

[2] K. Sayood, H. H. Otu, and N. Demir, "Joint source/channel coding for variable length codes," *IEEE Trans. on Communications*, vol. 48, no. 5, pp. 787–794, May 2000.

[3] M. Park and D. J. Miller, "Joint source-channel decoding for variable-length encoded data by exact and approximate MAP sequence estimation," *IEEE Trans. on Communications*, vol. 48, no. 1, pp. 1–6, Jan. 2000.

[4] R. Bauer and J. Hagenauer, "Symbol-by-symbol MAP decoding of variable length codes," in *Proc. 3. ITG Conf. on Source and Channel Coding*, Munich, Germany, Jan. 2000, pp. 111–116.

[5] E. Fabre, A. Guyader, and C. Guillemot, "Joint source-channel turbo decoding of VLC-coded Markov sources," in *Proc. IEEE Int. Conf. Acoust., Speech, Signal Processing*, Salt Lake City, UT, USA, May 2001, pp. 2657–2660.

[6] L. R. Bahl, J. Cocke, F. Jelinek, and J. Raviv, "Optimal decoding of linear codes for minimizing symbol error rate," *IEEE Trans. on Information Theory*, pp. 294–287, Mar. 1974.

[7] J. Kliewer and N. Goertz, "Soft-input source decoding for robust transmission of compressed images using two-dimensional optimal estimation," in *Proc. IEEE Int. Conf. Acoust., Speech, Signal Processing*, Salt Lake City, UT, USA, May 2001, pp. 2565–2568.

[8] J. Hagenauer, E. Offer, and L. Papke, "Iterative decoding of binary block and convolutional codes," *IEEE Trans. on Information Theory*, vol. 42, no. 2, pp. 429–445, Mar. 1996.

[9] N. Goertz, "On the iterative approximation of optimal joint source-channel decoding," *IEEE Journal on Selected Areas in Communications*, vol. 14, no. 9, pp. 1662–1670, Sept. 2001.

[10] D. Divsalar and F. Pollera, "Turbo codes for PCS applications," in *Proc. IEEE International Conference on Communications*, Seattle, WA, USA, June 1995, pp. 54–59.